

ELASTIC/PLASTIC SEPARATION ENERGY RATE
FOR CRACK ADVANCE IN FINITE GROWTH STEPS

A. P. Kfoury* and J. R. Rice**

ABSTRACT

A Griffith-type energy balance for crack growth leads to paradoxical results for solids that are modelled as elastic/plastic continua, since such solids provide no energy surplus in continuous crack advance to equate to work of separation [1]. An alternative proposed recently is that the finite size of the fracture process zone be taken into account, and a simple way of doing this is to define a crack tip energy release rate G^{Δ} based on the work of quasi-static removal of stresses from the prospective crack surfaces over a finite crack growth step Δa [2]. Recent finite element results for energy releases during crack growth are reviewed in this way and an analytical solution, based on the Dugdale-Bilby-Cottrell-Blinden (DBCS) crack model, is developed for G^{Δ} when Δa is small compared to plastic zone size. This solution and the finite element results are in remarkably good agreement and, based on the analytical solution, we develop the asymptotic formula for the value of the J integral required for crack growth, $J = .70 \zeta \exp(.43/\zeta) G^{\Delta}$, with $\zeta = (1-\nu^2)\sigma_y^2 \Delta a / E G^{\Delta}$, and this formula is valid whenever ζ is smaller than, approximately, 0.15; σ_y is the yield stress. A defect of the DBCS model, however, is that unlike the finite element results, it makes no distinction between the criterion for onset of growth and that for continuing growth in the case of highly brittle solids.

INTRODUCTION

Recent work in elastic/plastic crack mechanics has been successful in identifying "characterizing parameters" (J, δ_t) for the crack tip deformation field, and the condition for onset of growth from a pre-crack can be phrased in terms of these. But no similar characterizing parameter has yet been identified for stably growing cracks. Indeed, it seems likely that no useful general parameter exists, defined independently of the fine-scale details of the crack tip deformation field. Thus it appears to be necessary to have some kind of model of the crack tip separation process, on which to found a suitable approach to crack growth. Such a model, while necessarily limited in respect to how closely actual separation processes could be described, would nevertheless lead to definite predictions of conditions necessary for the onset of growth, as well as those for stable growth to exist at all and for stable growth to give way to a terminal, running fracture instability.

The first inclination might be to generalize the Griffith approach by assuming that the non-ideally brittle material has some characteristic work of separation, per unit new crack area, and that this is to be equated

*Department of Engineering, University of Cambridge, Cambridge, England

**Division of Engineering, Brown University, Providence, R.I., U.S.A.

at the critical condition to the surplus of work done on the material, by external loads, over the energy stored or dissipated by stress working during a unit increase in crack area. A tacit assumption in such an approach is that the energy transfers can be decoupled, in a manner that calculation of the energy surplus can be based on the mathematical solution for a crack cut continuously ahead in whatever continuum model (elastic, elastic/plastic, viscoelastic, etc.) is considered representative of the material at hand.

For perfectly elastic materials, the Griffith approach seems quite suitable, at least to the neglect of certain lattice effects, and essentially exact agreement is obtained between it and a singularity-free model of the crack end zone, in the spirit of the Barenblatt model, but in which a definite relation between restraining stress and separation displacement is assumed to apply in a small but finite crack tip cohesive zone [3].

But the temptation to generalize the Griffith approach for other continua must be avoided. Rice [1] has shown that serious paradoxes arise for elastic/plastic materials; when stress-strain relations for these entail the saturation of flow stress to a finite value of large strain, it is evident that there is no singularity in recoverable energy density at the crack tip, and one may then prove that there is zero surplus of work done by external loads over stress working on the deformation of material elements. Hence fracture according to the attempted generalization of the Griffith model cannot occur in such a material.

Recently Kfoury and Miller [2] confirmed this behavior in an elastic/plastic finite element solution for a growing crack. More significantly, however, they also suggested a way in which an energy balance concept could be used to model crack growth, but in a manner which involves only rather simple calculations from the standpoint of numerical solution methods. The method recognizes explicitly that there is some finite size scale associated with the crack tip separation process and therefore computes, at the continuum level, the work done in quasi-statically and proportionally reducing to zero the stresses which act over a finite growth step size Δa ahead of the crack. This distance is considered characteristic of the material and, if $-\Delta W$ is the work of unloading the initially stressed segments of crack wall, per unit length along the crack front, then the separation energy rate is defined by

$$G^{\Delta} \equiv \frac{\Delta W}{\Delta a} \quad (1)$$

For crack growth G^{Δ} must equal the work required for separation, namely G_C^{Δ} , which is also considered characteristic of the material.

Note that for elastic materials G^{Δ} is essentially independent of Δa , when Δa is sufficiently small, and hence it is appropriate to take the limit $\Delta a \rightarrow 0$. But elastic/plastic materials give $G^{\Delta} \rightarrow 0$ in this same limit, by Rice's result [1]. Particularly, the issue here is the size of Δa in relation to the size of the plastically deforming region at the crack tip.

In the present work, we leave open the question of how physically appropriate such an approach is as a model of the fracture process. It is obvious that one can have models at various levels of complexity, and this one may have its limitations. It is, perhaps, the simplest workable approach among the class of models which might, loosely, be described as "energy balance" or "cohesive zone" models. Certainly, it has the virtue of being easy to employ in calculations, and some promising results based on it have

been demonstrated by Kfoury and Miller [2] for low-temperature cleavage fractures of steels.

The finite element results of Kfoury and Miller [2, 4] are briefly reviewed and discussed in the present framework in the next section. Following that, we carry out the analytical calculation of G^{Δ} for the DBCS crack yield model and compare results with the numerical calculations. We find these to be mutually reinforcing, in that the general trend of G^{Δ} with Δa , predicted numerically, is well-matched by the analytical calculation. Further, the analytical calculation suggests the proper asymptotic form of the variation of G^{Δ} with Δa when the latter is small in comparison to plastic zone dimension. In this way, our calculation here allows the extrapolation of numerical solutions into a range well beyond what it is feasible to compute economically by finite elements.

We note in passing that paradoxes in energy balance approaches to fracture criteria arise in other models of continua, but that these likewise seem to be resolvable when the finite structure of the crack tip separation zone is accounted for in some manner. For example, Kostrov and Nikitin [5] show for linear viscoelastic solids that appropriate rate dependence of the crack growth criterion is not predicted from an energy balance based on a continuously advancing singular crack tip model, but that the problem is resolved with models that entail a Barenblatt finite cohesive zone at the crack tip. Also, Rice and Simons [6], in a recent solution for shear crack growth in a fluid-infiltrated porous elastic solid with coupling between deformation and Darcy fluid diffusion, demonstrate a similar paradox. Here the expected Griffith elastic result for the limiting case of rapid, undrained deformation is not obtained, but they show that the proper limit is established in a model that entails a finite shear breakdown zone at the fault tip. Since the linearized equations of porous media are precisely analogous to those of linear coupled thermoelasticity, this suggests also that there will be a similar paradox for a thermoelastic material model at the limit of rapid isentropic deformation, although the difference between isothermal and isentropic moduli for most solids is too small to make the effect significant numerically.

CRACK TIP FINITE-ELEMENT NODE RELEASE METHOD

Kfoury and Miller [2, 4] carried out an elastic/plastic analysis on the center cracked plate in plane strain, shown in Figure 1. The plate was loaded at the boundaries by an applied stress σ_p normal to the crack and a lateral applied stress σ_Q parallel to the crack. Here, only the uniaxial mode $\sigma_Q = 0$ will be considered. The properties of the von Mises material are also given in Figure 1.

Elastic loading up to incipient yielding at the crack tip was followed by incremental loading to several applied load levels corresponding to different crack tip plastic zone sizes. For each load level a crack tip node release technique was used at constant applied stress to calculate the crack separation energy rate. Four crack tip nodes were released successively and the energy rate was evaluated for each release. Figure 2 shows a typical plastic zone size developed during the initial loading stage before crack extension has taken place and Figure 2b shows the same material at the same load after the four crack tip node releases. The computer-drawn deformations are exaggerated by a factor of 50. The initial and extended crack profiles corresponding to the next higher applied load level are shown in Figure 3 on which the elliptical profile for an elastic

material has also been drawn. Note the blunted crack tip associated with the $1/r$ type strain singularity [3,7] before crack extension and the sharper crack profile associated with the $\log(1/r)$ type strain singularity [7,8] after crack extension has taken place. The equivalent plastic strains in the immediate vicinity of the crack tip were, for the static crack, about twice the corresponding value when the crack had extended.

The crack separation energy rate G^Δ can be computed by imagining that the surfaces are held together over distance Δa by an imposed stress field in equilibrium with the applied loads and constraints. Assign to the imposed stress field a load factor, initially unity, and gradually reduce the load factor to zero so that the surfaces at Δa are released quasi-statically at constant applied load. Calling ΔW the energy absorbed during the crack opening, G^Δ is computed from (1).

The crack separation energy rate is intended to measure the energy available to separate the surfaces over Δa . Since the growth step Δa is assumed small compared to the average body dimensions, e.g., the half crack length a , in an elastic material G^Δ is sensibly equal to the Griffith energy release rate G where

$$G = J = - \frac{\partial P}{\partial a} \quad (2)$$

and P is the potential energy, i.e., the sum of the potential energy of the applied forces, σ_p and σ_0 , and the strain energy, and J is the path independent contour integral [3]. If the material is linear elastic, we have further,

$$G^\Delta = G \approx (1-\nu^2) K_I^2 / E \quad (3)$$

where K_I is Irwin's mode I stress intensity factor and E and ν are Young's modulus and Poisson's ratio for the material.

Dependence of G^Δ on crack tip plastic zone size

For an elastic-plastic material in small scale yielding, the crack tip plastic zone size is proportional to $(K_I/\sigma_y)^2$, where σ_y is the yield stress in a uniaxial tensile test. Thus the ratio of jump step over plastic zone size is proportional to

$$S \equiv (\sigma_y/K_I)^2 \Delta a$$

The analysis shows that at the same value of the applied load, G^Δ decreases and eventually vanishes as S decreases towards zero, as predicted on general grounds [1]. This is illustrated in Figure 4. At the other end of the scale, for the largest value of $S = 0.457$, G^Δ is essentially equal to J or G for the elastic material.

Figure 4 also gives values of J/G at different values of S . Note that for values of S larger than 0.071, J/G is less than 1.05 but the ratio J/G rises rapidly when S is less than 0.071, indicating deviations from "small scale yielding" conditions for this geometry. Here J as used is always defined as the contour integral taken in the elastic zone, and we subsequently will normalize results with J rather than G as a means of accounting, at least approximately, for large scale yielding effects.

A somewhat different measure of ductility, analogous to S , but which arises in our later calculations and involves only those properties which are

considered characteristic of the material, is given by

$$\zeta = \frac{(1-\nu^2)\sigma_y^2 \Delta a}{EG^\Delta} \quad (4)$$

The relations in Figure 4 can be presented in terms of ζ in the form

$$\frac{J}{G^\Delta} = \chi(\zeta) \quad (5)$$

Figure 5 gives the ζ, χ dependence.* When $\zeta = 0.457$ the material response is linear (this figure may vary a little according to the finite element mesh on which the results are based) and $J = G^\Delta$. When ζ is very small J/G^Δ becomes very large. A brittle to ductile transition value [2] for ζ can be defined, approximately, as $\zeta_t \approx 0.091$.

Fracture criterion

The ζ, χ curve can be used to represent dependence of the critical value J_{IC} on G_c^Δ when the fracture criterion for crack extension is $G^\Delta = G_c^\Delta$. Here G_c^Δ is the critical value of G^Δ for the material in the current state. The plausible assumption was made in [2] that G_c^Δ and Δa are constant in the considered range corresponding to values of ζ larger than ζ_t ; these values can represent the states of a material at different temperatures within a temperature range varying from the transition temperature T_t to a very low temperature T_b corresponding to nil reduction in area in a uniaxial tensile test, assuming that only the plastic flow properties, but not Δa or G_c^Δ , vary with T . The critical value of G_c^Δ was taken to be G_{cb} , i.e., G_{IC} at the temperature T_b . Then, from (3)

$$G_{cb} = \frac{(1-\nu^2) K_{Icb}^2}{E} \quad (6)$$

where K_{Icb} is the fracture toughness at the temperature T_b . While thus far examined experimentally only in relation to data on cleavage in steels [2], the same concepts may be useful, with suitably chosen G_c^Δ and Δa , for more ductile mechanisms of crack growth.

'Initial condition' curve and steady crack growth

Very large plastic strains which cause the tip to blunt are generated during the initiation process and are concentrated in a small region in the immediate vicinity of the crack tip. The associated initial stresses were found to have a short range effect on G^Δ ; only the first tip node release values were affected in the considered χ range ($\chi < 4.54$). The solid ζ, χ curve in Figure 5 represents the 'steady condition' values obtained from the average values of G^Δ/a , calculated from the last three tip node releases at a given load level. For plastic zone sizes corresponding to $\chi > 3.35$, the values of G^Δ/a calculated from the first crack tip node release were larger than the averages for the next three node releases and

* ζ and χ are related to the parameters ϕ and ψ in [2] by

$$\zeta = .457/\phi, \quad \chi = J\psi/G\phi.$$

were used to describe the 'initial condition' curve shown dotted in Fig. 5. The difference between the initial and steady condition curves is also a reflection of the varying crack profiles and associated types of strain singularities mentioned earlier, as the crack penetrates into the plastic zone. Consider a material in a state given by $\zeta = .10$, say, and let an increasing load be applied, represented by an upward vertical displacement of the state point in the ζ, χ plane. When the 'initial condition' is reached the crack begins to move but as soon as it has penetrated a short distance into the plastic zone, the 'initial condition' curve is no longer applicable. As the load is increased further steady crack growth takes place and instability occurs only when the solid curve is reached. For values of ζ larger than 0.127, catastrophic failure is not preceded by steady crack growth, according to the present model, since the solid curve is the first to be reached.

Thus the results suggest the occurrence of stable crack growth in sufficiently ductile materials (ζ small) but not in more brittle materials.

G^{Δ} CALCULATION FOR THE DBCS CRACK MODEL

Here the DBCS model is employed as a basis for the calculation of G^{Δ} in the ductile range, say $\zeta < 0.15$, which corresponds to a step Δa of small size compared to the plastic zone dimension. The model is, of course, a very much simplified representation of crack tip yielding but, as will be seen, it enables the calculation of a simple formula relating J to G^{Δ} which is in remarkably good agreement with the finite element results and enables their extrapolation to a range which could not economically be computed. Figure 6 shows the model and, to simplify the calculations, we follow Rice's ([7], p. 264) small scale yielding formulation in which the crack is viewed as being, effectively, semi-infinite with asymptotic approach to a surrounding elastic singular field of intensity factor K . The crack surfaces are held together within the plastic zone, of size ω_0 before the crack advance, by the uniform stress Y . The stress Y is expected to lie between the tensile yield stress σ_y and the Prandtl field stress [3] $3\sigma_y$ on account of the triaxiality and hydrostatic effects; it is generally agreed that a value in the neighborhood of $2\sigma_y$ is necessary to make the crack tip opening displacement of this model coincide with more exact predictions. A close estimate of Y will be obtained later by comparing the model with the finite element one.

Since the material is linear elastic for the purpose of computing the stresses and displacements, solutions for different loadings can be superimposed. The singularity of strength K , caused by the applied loading, must be cancelled by an equal and opposite singularity K' resulting from the stresses Y , so that a bounded stress results ahead of the crack tip. Thus

$$K_{\text{net}} = K + K' = 0 \quad (7)$$

The value of K' is obtained by using the solution for a point load $p(r)dr$ on the crack surface ([7], eq. 98),

$$K' = (2/\pi)^{1/2} \int_0^{\infty} r^{-1/2} p(r) dr = - (2/\pi)^{1/2} Y_0^{\omega_0} r^{-1/2} dr,$$

and from (7)

$$K = -K' = \frac{2\sqrt{2}}{\sqrt{\pi}} Y \sqrt{\omega_0} \quad (8)$$

determines the plastic zone dimension ω_0 as

$$\omega_0 = \frac{\pi K^2}{8 Y^2} \quad (9)$$

The total separation between the upper and lower crack (or plastic zone) surfaces is denoted by δ , and this is expressed by superimposing the effect of the applied loading and of the stresses Y to obtain

$$\delta = 8 \frac{K}{E'} \left(\frac{r}{2\pi} \right)^{1/2} - \frac{Y}{E'} \omega_0 f \left(\frac{r}{\omega_0} \right)$$

Here $E' = E/(1-\nu^2)$ and the function $f(\dots)$ arises from the solution for uniform loading of crack surfaces adjacent to the tip. This function contains a term which varies as $r^{1/2}$, and which is cancelled by the first term in the equation for δ so that the net effect is smooth closure of the plastic zone surfaces at $r = 0$. Thus the expression for δ can be put in the form

$$\delta = \frac{Y}{E'} \omega_0 g \left(\frac{r}{\omega_0} \right) \quad (10)$$

and the function $g(\dots)$ is given by ([7], eq. 223)

$$g(\lambda) = \frac{8}{\pi} \left[\sqrt{\lambda} - \frac{1}{2} (1-\lambda) \log \left(\frac{1+\sqrt{\lambda}}{|1-\sqrt{\lambda}|} \right) \right] \quad (11)$$

Calculation of separation energy

The growth step is assumed to be smaller than the yield zone size ω_0 . As the crack tip release over Δa begins, Figure 7a, the stress Y acts over a distance $\omega (= \omega_0 - \Delta a)$, initially) and a stress $\sigma (= Y)$, initially) acts over Δa . During the release, Figure 7b, σ varies quasi-statically from Y to 0, and ω from $\omega_0 - \Delta a$ to ω_0 again when full release has taken place. As illustrated, we assume proportional release of the stresses acting over Δa in the calculation; the final result for G^{Δ} will, of course, be dependent on particular details of the release process.

By a similar argument to that used previously and by decomposing the stresses into σ acting over $\omega + \Delta a$ and $(Y - \sigma)$ acting over ω , we get

$$K_{\text{net}} = K - \frac{2\sqrt{2}}{\sqrt{\pi}} \sigma \sqrt{\omega + \Delta a} - \frac{2\sqrt{2}}{\sqrt{\pi}} (Y - \sigma) \sqrt{\omega} = 0$$

Thus, using (8),

$$Y \sqrt{\omega_0} - \sigma \sqrt{\omega + \Delta a} - (Y - \sigma) \sqrt{\omega} = 0 \quad (12)$$

Also, by the same argument as used previously, the displacement distribution δ during the release process is given by

$$\delta = \frac{\sigma}{E'} (\omega + \Delta a) g \left(\frac{r}{\omega + \Delta a} \right) + \frac{Y - \sigma}{E'} \omega g \left(\frac{r}{\omega} \right) \quad (13)$$

where r is as defined in Figure 7b and $g(\dots)$ is the same function as in equations (10,11).

As illustrated in Figure 7b, we let $\Delta\delta$ be the displacement given by (13) minus the displacement given by (10), so that $\Delta\delta$ is the alteration in opening of the plastic region during the load release process. Hence, at some material point at distance x ahead of the initial crack tip,

$$\Delta\delta = \frac{\sigma}{E'} (\omega + \Delta a) g\left(\frac{\omega + \Delta a - x}{\omega + \Delta a}\right) + \frac{Y - \sigma}{E'} \omega g\left(\frac{\omega + \Delta a - x}{\omega}\right) - \frac{Y}{E'} \omega_0 g\left(\frac{\omega_0 - x}{\omega_0}\right) \quad (14)$$

Now the crack separation energy rate as defined by (1) is

$$G^\Delta = \frac{1}{\Delta a} \int_{x=0}^{x=\Delta a} \left[\int_{\sigma=Y}^{\sigma=0} \sigma d(\Delta\delta) \right] dx \quad (15)$$

Noting that $\sigma d(\Delta\delta) = d(\sigma\Delta\delta) - (\Delta\delta)d\sigma$, and observing that $\sigma\Delta\delta$ vanishes at both limits on σ , this can be rewritten as

$$G^\Delta = \frac{1}{\Delta a} \int_{x=0}^{x=\Delta a} \int_{\sigma=0}^{\sigma=Y} \Delta\delta d\sigma dx = \frac{1}{\Delta a} \int_{x=0}^{x=\Delta a} \int_{\omega=\omega_0}^{\omega=\omega_0 - \Delta a} \Delta\delta \frac{d\sigma}{d\omega} d\omega dx \quad (16)$$

where in the last form of the integral, we recognize that σ can be written as a function of ω from (12). In fact, the relation is

$$\sigma = Y \frac{\sqrt{\omega_0} - \sqrt{\omega}}{\sqrt{\omega + \Delta a} - \sqrt{\omega}}, \text{ and} \quad (17)$$

$$\frac{d\sigma}{d\omega} = -\frac{Y}{2} \frac{\sqrt{\omega + \Delta a} + \sqrt{\omega} - \sqrt{\omega_0}}{\sqrt{\omega} \sqrt{\omega + \Delta a} (\sqrt{\omega + \Delta a} - \sqrt{\omega})} \quad (18)$$

At this point we insert (17) for σ where it appears in the expression (14) for $\Delta\delta$, and then insert $\Delta\delta$ and $d\sigma/d\omega$, from (18), into the integrand in (16); these steps express the integrand in terms of the variables of integration, x and ω . The final result is rather complicated and to simplify its presentation we introduce the dimensionless step size $\epsilon = \Delta a/\omega_0$, we define $X = x/\omega_0$ and $Z = 1 - \omega/\omega_0$, and we note from (9) that

$$\frac{Y^2 \omega_0}{E'} = \frac{\pi}{8} \frac{K^2}{E'} = \frac{\pi}{8} J, \quad (19)$$

where the small scale yielding context of the DBCS analysis justifies writing K^2/E' as J . Then the energy release rate can be written as

$$G^\Delta = J \int_0^\epsilon \int_0^\epsilon F(X, Z; \epsilon) dZ dX \quad (19)$$

where the function F is

$$F(X, Z; \epsilon) = \frac{\pi}{16\epsilon} \left[\frac{1 - \sqrt{1-Z}}{\sqrt{1+\epsilon-Z} - \sqrt{1-Z}} (1+\epsilon-Z) g\left(\frac{1+\epsilon-Z-X}{1+\epsilon-Z}\right) + \frac{\sqrt{1+\epsilon-Z} - 1}{\sqrt{1+\epsilon-Z} - \sqrt{1-Z}} (1-Z) g\left(\frac{1+\epsilon-Z-X}{1-Z}\right) - g(1-X) \right] \times \left[\frac{\sqrt{1+\epsilon-Z} + \sqrt{1-Z} - 1}{\sqrt{1-Z} \sqrt{1+\epsilon-Z} (\sqrt{1+\epsilon-Z} - \sqrt{1-Z})} \right], \quad (20)$$

and where the function $g(\dots)$ on which it depends is defined by (11).

Asymptotic formula for small step size, $\epsilon = \Delta a/\omega_0 \ll 1$

Equation (19) as derived is valid for all $\epsilon \leq 1$, but here we are primarily interested in the result for small growth steps, by comparison to plastic zone size, and thus it is appropriate to develop an asymptotic expression of (19) for the small ϵ range. Note in this case that we are always interested in knowing the function $g(\dots)$ when its argument is in the neighborhood of unity, and in that case (11) leads to

$$g(1+u) = \frac{8}{\pi} \left[1 + \frac{1}{2} u \log \frac{1}{|u|} + \frac{1}{2} u \log(4e) + \dots \right] \quad (21)$$

where e is the natural logarithm base and where the neglected terms are of the order $u^2 \log|u|, u^2$, etc. Using this expression in (20) for $F(X, Z; \epsilon)$ and noting that X and Z , as they enter the integrand in (19), are of the same order as ϵ , the function F has the expansion

$$F(X, Z; \epsilon) = \frac{1}{2\epsilon^3} \left\{ (\epsilon-Z) \left[X \log \frac{1}{X} + (\epsilon-X) \log \frac{1}{\epsilon-X} \right] \times \left(1 + \frac{\epsilon-ZZ}{4} \right) + \epsilon (\epsilon-Z) \log(4e) + \dots \right\} \quad (22)$$

where the neglected terms within the large bracket are of order $\epsilon^3, \epsilon^4 \log \epsilon$, etc.

By substituting this expression for F into (19) and performing the integrations on X and Z , we now find that

$$G^\Delta = \frac{1}{4} J \left[\epsilon \log \frac{1}{\epsilon} + \left(\frac{3}{2} + \log 4 \right) \epsilon - \frac{1}{3} \epsilon^2 \log \frac{1}{\epsilon} + \dots \right] \quad (23)$$

where now the neglected terms are of order $\epsilon^2, \epsilon^3 \log \epsilon$, etc.

Discussion of the result (23)

First, we observe that as the step size $\epsilon = \Delta a/\omega_0$ approaches zero in (23), we do indeed obtain the anticipated [1] null energy surplus, $G^\Delta = 0$. But for ϵ small yet finite, say $\epsilon < 0.20$, it suffices to retain only the first two terms within the bracket of (23), namely

$$G^{\Delta} = \frac{\epsilon}{4} J \left(\log \frac{1}{\epsilon} + 2.886 \right) \quad (24)$$

where $2.886 = 3/2 + \log 4$.

A more useful point of view is to consider Δa and G^{Δ} as given quantities, characteristic of the material, and to solve for J in terms of them. To do so we write the DBCS effective yield stress parameter Y as $C\sigma_y$, where C is a constant to be chosen to fit the DBCS model to more exact plane strain elastic-plastic solutions, and we note from (9) that

$$\epsilon \equiv \frac{\Delta a}{\omega_0} = \frac{8}{\pi} \frac{Y^2}{K^2} \Delta a = \frac{8C^2}{\pi} \frac{(1-\nu^2) \sigma_y^2 \Delta a}{E J}$$

This may be re-expressed in terms of $\zeta = (1-\nu^2) \sigma_y^2 \Delta a / EG^{\Delta}$, the dimensionless step size parameter introduced in equation (4) and used in Figure 5. In particular,

$$\epsilon = \frac{8C^2}{\pi} \frac{G^{\Delta}}{J} \zeta, \quad (25)$$

and upon insertion of this into equation (24) we may solve for J as

$$J = \frac{8C^2}{\pi} \zeta \exp \left(\frac{\pi}{2C^2\zeta} - 2.886 \right) G^{\Delta}. \quad (26)$$

DISCUSSION

Equation (26) from the DBCS analysis can be rewritten in the form

$$\log \left(\frac{\pi}{8\zeta} \frac{J}{G^{\Delta}} \right) = \frac{\pi}{2C^2} \frac{1}{\zeta} - 2.886 + \log C^2. \quad (27)$$

Thus the left side of this equation, when plotted against $1/\zeta$, gives a straight line, and the result is valid when ζ is small (or $1/\zeta$ large). Further, if the finite element results are to agree with the simple formula (27), based on the DBCS model, then they too should plot onto a straight line for large $1/\zeta$.

In Figure 8 we have plotted the left side of (27) according to the finite-element results, versus $\pi/2\zeta$, using all the computed points (crosses) defining the "steady condition" curve in Figure 5. It is seen that the points corresponding to large values of $1/\zeta$ (say, for $\zeta < 0.15$) are fit excellently by a straight line relation. Further the slope of the best fitting straight line defines, according to (27), the value of $1/C^2$. This we find to be 0.275, so that $C = 1.91$ and thus

$$Y = C\sigma_y = 1.91 \sigma_y. \quad (28)$$

From what has been noted earlier, this is a very reasonable value for matching the DBCS model to more exact plane strain analyses.

The horizontal axis intercept in Figure 8 is at 4.704 so that the straight line drawn through the finite element results has the equation

$$\begin{aligned} \log \left(\frac{\pi}{8\zeta} \frac{J}{G^{\Delta}} \right) &= 0.275 \left(\frac{\pi}{2\zeta} - 4.704 \right) \\ &= (0.275) \frac{\pi}{2\zeta} - 2.585 + \log (1/0.275). \end{aligned} \quad (29)$$

Comparing this with equation (27) and recognizing that $C^2 = 1/0.275$, we see that even the DBCS constant term 2.886 of equations (26) and (27) is fairly well matched by the finite-element results, the latter being best fit by the term 2.585.

Finally, writing equation (29) in the same form as (26) we obtain

$$J = 0.698 \zeta \exp (0.432/\zeta) G^{\Delta}, \quad (30)$$

and this is evidently a close mathematical description of the solid curve through the finite element results in Figure 5 for small ζ . If the DBCS term 2.886 were used instead of the best-fit term 2.585, e.g. as in equation (26), the effect would be to reduce the pre-exponential term in (30) to 0.517, with no change of the exponential term.

One important aspect of the finite element results, not reproduced in the DBCS model, is that there is a distinction between G^{Δ} for the first crack growth step and that for subsequent steps (compare the "initial condition" and "steady condition" curves in Figure 5). This suggests that a critical G^{Δ} criterion, with associated step size parameter ζ of (4), provides a framework that will predict some amount of stable crack growth, following initiation, in sufficiently ductile materials (say, those with $\zeta < 0.12$). The failure of the DBCS model to predict this is a serious shortcoming since experiments on pre-cracked ductile metal specimens are well known to show some stable crack growth.

If the somewhat arbitrarily chosen transition value $\zeta_t = 0.091$ shown in Figure 5 is used in equation (30), we compute that

$$\frac{J_t}{G_c} \approx \left(\frac{K_{Ict}}{K_{Icb}} \right)^2 = 7.18 \implies K_{Ict} \approx 2.7 K_{Icb}. \quad (31)$$

Here, for a material with temperature-dependent yield stress (but G_c^{Δ} and Δa assumed T -independent, [2]), K_{Icb} is the toughness at some low temperature T_b for which J is essentially equal to G_c^{Δ} at fracture, because the yield zone size is small compared to the fracture step size Δa . Thus if K_{Icb} is used to compute G_c^{Δ} through the usual elastic fracture mechanics formula (3), then by establishing the yield stress σ_{yt} at the temperature T_t for which $K_{Ic} = 2.7 K_{Icb}$, and assuming that this corresponds to $\zeta = \zeta_t = 0.091$, the step size Δa associated with the experimental data can be calculated from (4) as

$$\Delta a = 0.091 K_{Icb}^2 / \sigma_{yt}^2. \quad (32)$$

(This is an alternative to a method suggested previously [2] based on determining σ_{yb} at the temperature T_b . Note that $(\sigma_{yb}/\sigma_{yt})^2 \approx 5$). Of course the method assumes that a temperature T_b for which $J \approx G_c^\Delta$ at fracture actually exists; it may not in some cases, and then G_c^Δ and Δa must be determined through a more elaborate fit to the results in Figure 5.

Also, it seems possible that in many cases, for example when ductile hole growth mechanisms are operative at the crack tip, G_c^Δ should be related to σ_y and other plastic flow properties, and hence be T dependent if the flow properties are T dependent. Further, there could then be an indirect T dependence of Δa , in the sense that the density and thus the spacing of hole nucleation sites could depend on the general stress levels, which are proportional to σ_y , prevailing very near the crack tip.

CONCLUSIONS

A simple means of resolving the energy balance paradox in elastic/plastic materials is to base the crack growth criterion on the separation energy rate G_c^Δ defined in relation to a finite growth step Δa . The behavior of the DBCS strip model in this context agrees well with that of the finite-element model, and together they provide a rational basis for relating the J value for crack growth to G_c^Δ and Δa in the transitional regime, say $\zeta < 0.15$. Still, a defect of the DBCS model is its lack of prediction of stable crack growth. The approach provides a promising basis for explaining cleavage toughness transitions in materials with temperature-dependent plastic flow properties, but its applicability to more ductile fracture mechanisms is not yet much explored. The use of this approach for the description of stable crack growth in ductile materials (small ζ) also requires further study. Further, it remains an open issue to relate the parameters G_c^Δ and Δa of the model to microscale fracture processes as revealed fractographically.

ACKNOWLEDGEMENT

This study was carried out at Brown University under support of the NSF Materials Research Laboratory. A.P.K. was also partly supported by the University of Cambridge, and the UK Science Research Council sponsored the finite-element investigations cited.

REFERENCES

1. RICE, J. R., Proceedings First International Conference on Fracture, Sendai, ed. T. Yokobori et al., Jap. Soc. Strength and Fracture of Materials, Tokyo, 1, 1966, 309.
2. KFOURI, A. P. and MILLER, K.J., Crack separation energy rates in elastic-plastic fracture mechanics, submitted to Proc. Inst. Mech. Eng. (London), 1976.
3. RICE, J.R., Trans. ASME J. Appl. Mech., 35, 1968, 579.
4. KFOURI, A.P. and MILLER, K.J., Int. J. Pres. Ves. and Piping, 2, 1974, 179.
5. KOSTROV, B.V. and NIKITIN, L.V., Arch. Mech. Stosowanej, 22, 1970, 749.
6. RICE, J.R. and SIMONS, D. A., J. Geophys. Res., in press, 1976.
7. RICE, J.R., Fracture, An Advanced Treatise, ed. H. Liebowitz, Academic Press, New York, 2, 1968, 191.
8. RICE, J.R., Mechanics and Mechanisms of Crack Growth (Proc. April 1973 Conf. at Cambridge, England), ed. M.J. May, British Steel Corp. (Phys. Met. Centre Publ.), 1975, 14.

Separation Energy Rate for Crack Advance

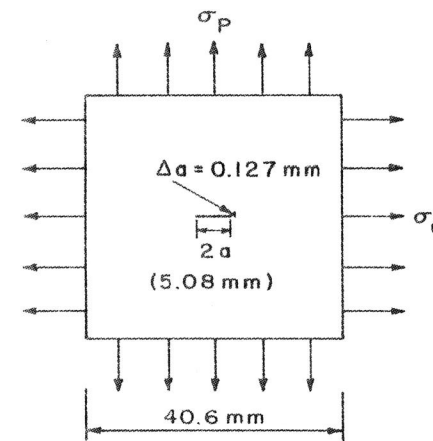
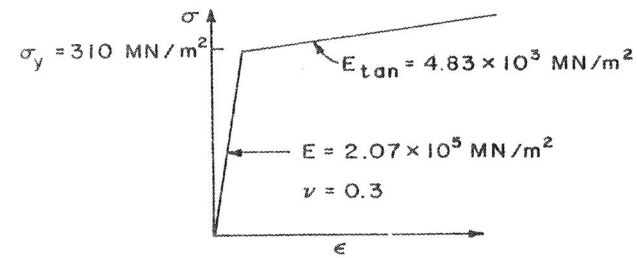


Figure 1 Center cracked plate in plane strain and (Mises) material properties, on which finite-element results are based

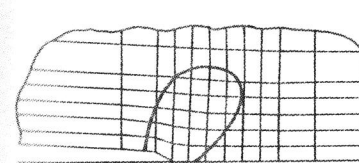


Figure 2a Plastic zone at $\sigma_p = 165.65 \text{ MN/m}^2$ before crack tip node releases. At incipient yielding, $\sigma_p = 54.14 \text{ MN/m}^2$.

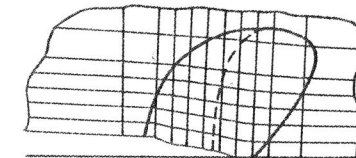


Figure 2b Plastic zone after four crack tip node releases at $\sigma_p = 165.65 \text{ MN/m}^2$. Dashed curve gives boundary of active plastic zone

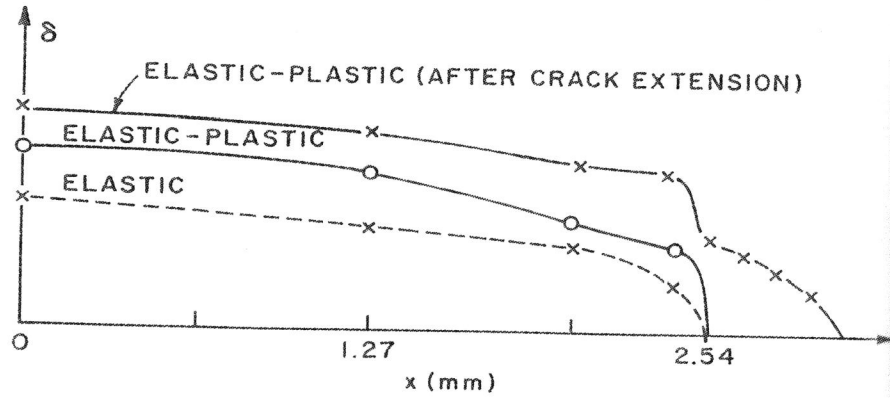


Figure 3 Half crack profiles before and after crack extension at $\sigma_p = 195.45 \text{ MN/m}^2$

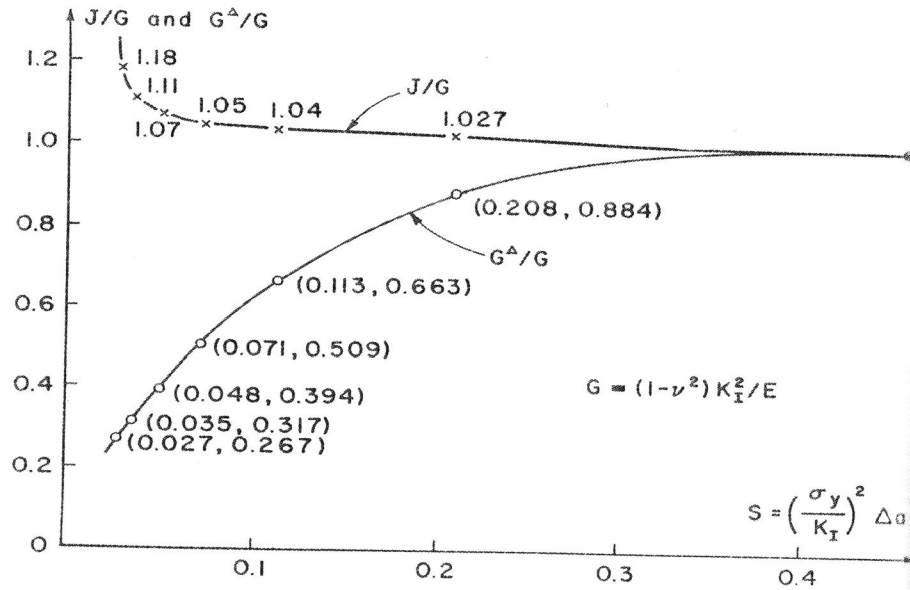


Figure 4 Variation of G^Δ and J with ratio of Δa to crack tip plastic zone size

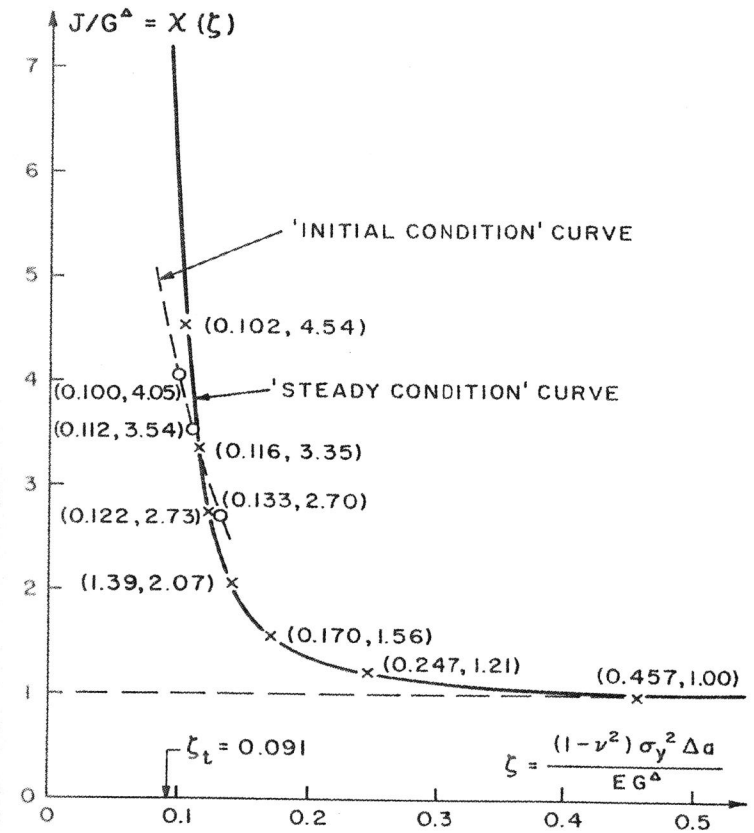


Figure 5 Dependence of J/G^Δ on ζ obtained from finite element model

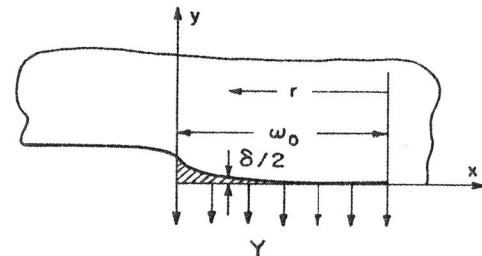


Figure 6 Dugdale-Bilby-Cottrell-Swinden strip yield model before crack extension

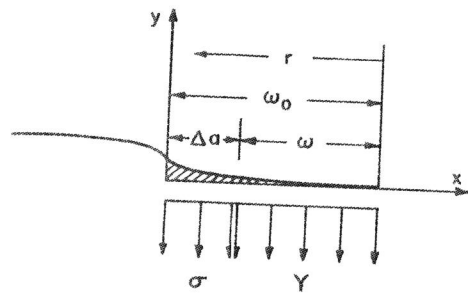


Figure 7a DBCS model at incipient crack opening

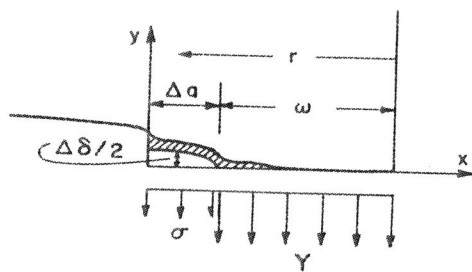


Figure 7b DBCS model during crack opening

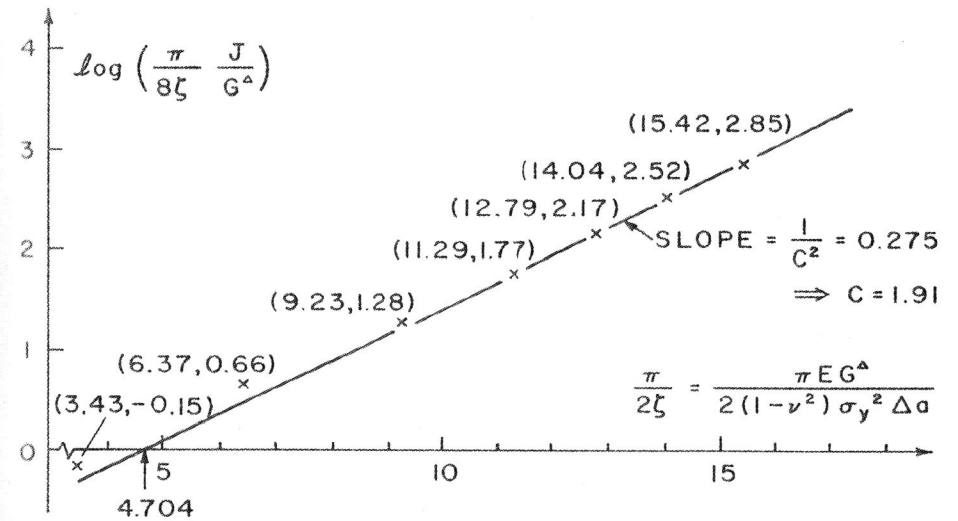


Figure 8 Plot of relation in form of equation (27) for DBCS strip model (solid line), using values (crossed points) obtained from finite element results for 'steady condition'